

# Modified bridgeless SEPIC for BLDC motor with ripple free input current

Surumi. S

M.Tech Student of MG University, Kerala, surumi2459@gmail.com

**Abstract**— A modified version of the bridgeless single-ended primary inductance converter (BL-SEPIC) as preferred to varying the speed of BLDC motor is presented in this paper. The conduction losses and ripple current in the input side of conventional SEPIC converter can be overcome by bridgeless SEPIC converter with auxiliary circuit. The performance of the system was analyzed through a MATLAB/Simulink model during discontinuous inductor current mode (DICM).

**Keywords**— SEPIC- Single Ended Primary Inductance Converter, PFC- Power Factor Correction

## INTRODUCTION

The Brushless DC (BLDC) motor is rapidly gaining popularity by its utilization in various industries, such as appliances, automotive, aerospace, consumer, medical, industrial automation equipment and instrumentation. A BLDC motor is known as a “synchronous” type because the magnetic field generated by the stator and the rotor revolve at the same frequency. One benefit of this arrangement is that BLDC motors do not experience the “slip” typical of induction motors. While the motors can come in one, two, or three phase types. As the name implies, the BLDC motors do not use brushes for commutation; instead they are electronically commuted[3]. BLDC motors have many advantages over brushed DC motors and induction motors, a few of these are,

- a. Better speed Vs torque characteristics
- b. High dynamic response
- c. High efficiency
- d. Long operating life
- e. Noiseless operation

Fig.1 shows the typical driving circuit for BLDC motor. The input circuit consists of a half wave or full wave bridge rectifier followed by a capacitor capable of maintaining a voltage of approximately the peak voltage of input sine wave until the next peak come along to recharge the capacitor. So the power factor will decrease. In such cases, active or passive power factor correction may be used to counteract the distortion and raise the power factor. Passive PFC uses a capacitive filter at the AC input to correct poor power factor. Passive PFC may be affected when environmental vibration occurs. Passive PFC requires that the AC input voltage be set manually. Passive PFC does not use the full energy potential of the AC line.

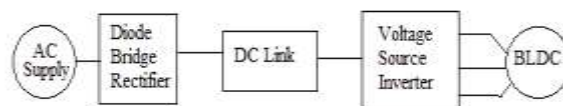


Fig.1 Typical driving circuit for BLDC motor

Many types of active power factor correction circuits are there buck converter, boost converter, buck-boost converter, conventional SEPIC converter, etc. Since, the input current of the PFC buck converter has dead angles during the time intervals when the input voltage is lower than the output voltage, there is a strong trade off between power factor and output voltage selection. On the other



Table. 1 switching sequence for 120 degree

Hall sensor position			Conducting Phases			Conducting switches					
A	B	C	A	B	C	S1	S2	S3	S4	S5	S6
1	0	0	+1	0	-1	1	1	0	0	0	0
1	1	0	0	+1	-1	0	1	1	0	0	0
0	1	0	-1	+1	0	0	0	1	1	0	0
0	1	1	-1	0	+1	0	0	0	1	1	0
0	0	1	0	-1	+1	0	0	0	0	1	1
1	0	1	+1	-1	0	1	0	0	0	0	1

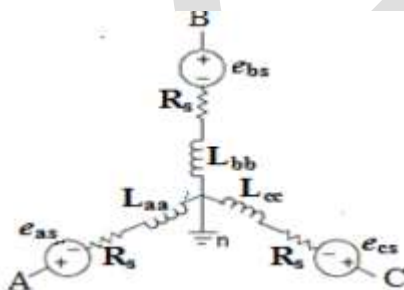


Fig. 4 Equivalent circuit

The system equation is given by,

$$\begin{bmatrix} v_{as} \\ v_{bs} \\ v_{cs} \end{bmatrix} = \begin{bmatrix} R_s & 0 & 0 \\ 0 & R_s & 0 \\ 0 & 0 & R_s \end{bmatrix} \begin{bmatrix} I_{as} \\ I_{bs} \\ I_{cs} \end{bmatrix} + p \begin{bmatrix} L_{aa} & L_{ab} & L_{ac} \\ L_{ba} & L_{bb} & L_{bc} \\ L_{ca} & L_{cb} & L_{cc} \end{bmatrix} \begin{bmatrix} I_{as} \\ I_{bs} \\ I_{cs} \end{bmatrix} + \begin{bmatrix} e_{as} \\ e_{bs} \\ e_{cs} \end{bmatrix}$$

Where,  $R_s$  is rotor resistance per phase,  $p$  is differential operator and  $e_{as}$ ,  $e_{bs}$  and  $e_{cs}$  are the induced emf. The induced emf is given by

$$e_{as} = k_b f_{as}(\theta_r) \omega_r \text{ (voltage)}$$

Where  $f_{as}$  is a unit function generator correspond to the trapezoidal induced emf as a function of rotor electrical position  $\theta_r$ .  $k_b$  is the emf constant and  $\omega_r$  rotor electrical speed.

$f_{as}$  is given by

$$\begin{aligned}
 f_{as}(\theta_r) &= (\theta_r) \frac{6}{\pi}, 0 < \theta_r < \frac{\pi}{6} \\
 &= 1, \frac{\pi}{6} < \theta_r < \frac{5\pi}{6} \\
 &= (\pi - \theta_r) \frac{6}{\pi}, \frac{5\pi}{6} < \theta_r < \frac{7\pi}{6} \\
 &= -1, \frac{7\pi}{6} < \theta_r < \frac{11\pi}{6}
 \end{aligned}$$

$$= (\theta_r - 2\pi) \frac{6}{\pi}, \quad 11\pi/6 < \theta_r < 2\pi$$

The electromagnetic torque ( $T_e$ ) is developed by the motor is given by

$$T_e = k_t \{ f_{as}(\theta_r) i_{as} + f_{bs}(\theta_r) i_{bs} + f_{cs}(\theta_r) i_{cs} \}$$

$$T_e = k_t \phi_{as} I_{as}$$

The electromechanical equation with the load is given by

$$Jp\omega_r + B\omega_r = (T_e - T_L)$$

where  $J$  is the moment of inertia,  $B$  is the friction coefficient and  $T_L$  is the load torque

$$\omega_r = \int (T_e - T_L - B\omega_r) / J dt$$

$$\theta_r = \int \omega_r dt$$

### B. Analysis of the proposed converter

The circuit diagram of the proposed bridgeless SEPIC with ripple-free input current as shown in fig.3 consists of the auxiliary circuit includes an additional winding  $N_s$  of the input inductor  $L_c$ , an auxiliary inductor  $L_s$ , and a capacitor  $C_a$ . The coupled inductor  $L_c$  is modelled as a magnetizing inductance  $L_m$  and an ideal transformer which has a turn ratio of  $1:n$  ( $n = N_s / N_p$ ). The leakage inductance of the coupled inductor  $L_c$  is included in the auxiliary inductor  $L_s$ . The capacitance of  $C_a$  is large enough, so  $C_a$  can be considered as a voltage source  $V_{Ca}$  during a switching period. Since the average inductor voltage should be zero at a steady state according to the volt-second balance law, the average capacitor voltage  $V_{Ca}$  is equal to the input voltage  $v_{in}$  during a switching period. Similarly, the average capacitor voltage  $V_{C1}$  is equal to  $v_{in}$ . Diodes  $D1$  and  $D2$  are the input rectifiers and operate like a conventional SEPIC PFC converter.  $DS1$  and  $DS2$  are the intrinsic body diodes of the switches  $S1$  and  $S2$ .

Fig. 4 shows the operating modes in the positive input voltage. Before  $t_0$ , the switch  $S1$  and the diode  $D_o$  are turned OFF and the switch  $S2$  is conducting. The input current is the sum of the freewheeling currents  $I_{s2}$  and  $I_{L2}$ [1].

#### Mode 1 [ $t_0, t_1$ ]:

At  $t_0$ , the switch  $S1$  is turned ON and the switch  $S2$  is still conducting. Since the voltage  $v_p$  across  $L_m$  is  $V_{in}$ , the magnetizing current  $i_m$  increases from its minimum value  $I_{m2}$  linearly with a slope of  $V_{in} / L_m$  as follows:

$$i_m(t) = I_{m2} + \frac{V_{in}}{L_m}(t - t_0). \quad \dots\dots\dots(1)$$

The voltage  $v_{Ls}$  across  $L_s$  is equal to  $(1-n)V_{in}$ . Therefore, the current  $i_s$  increases from its minimum value  $-I_{s2}$  linearly with a slope of  $(1-n)V_{in} / L_s$  as follows:

$$i_s(t) = -I_{s2} + \frac{(1-n)V_{in}}{L_s}(t - t_0). \quad \dots\dots\dots(2)$$

Since,

$$i_{in} = i_m + i_p = i_m - n i_s$$

The input current  $i_{in}$  can be written as follows,

$$i_{in}(t) = I_{m2} + n I_{s2} + \left( \frac{V_{in}}{L_m} - \frac{n(1-n)V_{in}}{L_s} \right) (t - t_0) \quad \dots\dots\dots(3)$$

From (3), the input current ripple can be cancelled out and  $i_{in}$  can be constant as  $I_{m2} + n I_{s2}$  by satisfying the following condition,

$$L_s = n(1-n)L_m \quad \dots\dots\dots(4)$$

#### Mode 2 [ $t_1, t_2$ ]

At  $t_1$ , the switch  $S_1$  is turned OFF and the switch  $S_2$  is still conducting. Since the voltage  $v_p$  across  $L_m$  is  $-V_o$ , the magnetizing current  $i_m$  decreases from its maximum value  $I_{m1}$  linearly with a slope of  $-V_o/L_m$  as follows

$$i_m(t) = I_{m1} - \frac{V_o}{L_m}(t - t_1) \dots\dots\dots(5)$$

The voltage  $v_{Ls}$  across  $L_s$  is  $-(1 - n)V_o$ , so that the current is decreases from its maximum value  $I_{s1}$  linearly with a slope of  $-(1 - n)V_o/L_s$  as follows

$$i_s(t) = I_{s1} - \frac{(1 - n)V_o}{L_s}(t - t_1) \dots\dots\dots(6)$$

From (5) and (6), the input current  $i_{in}$  can be written as follows,

$$i_{in}(t) = I_{m1} - nI_{s1} + \left( -\frac{V_o}{L_m} + \frac{n(1 - n)V_o}{L_s} \right) (t - t_1) \dots\dots\dots(7)$$

With the ripple-free condition of (4), the input current ripple in this mode can be cancelled out and  $i_{in}$  can be constant as  $I_{m1} - nI_{s1}$ .

**Mode 3 [t2, t0]**

At  $t_2$ , the current  $i_{Do}$  becomes zero, and the diode  $Do$  is turned OFF. Since  $i_{in} = i_m - n i_s = -i_s - i_{L1}$  in this mode, the input current  $i_{in}$  is the sum of freewheeling

Currents,  $I_{s2}$  and  $I_{L2}$  as follows,

$$i_{in} = I_{m2} + nI_{s2} = I_{s2} + I_{L2} \dots\dots\dots(8)$$

Since the average voltage across  $L_m$  should be zero under a steady state, the time ratio  $\Delta_1$  is obtained by

$$\Delta_1 = \frac{V_{in}}{V_o} D \dots\dots\dots(9)$$

Where,  $D$  is the duty cycle. In a switching period  $T_s$ , the maximum current of each inductor is rewritten as follows,

$$I_{m1} = I_{m2} + \frac{V_o}{L_m} \Delta_1 T_s \dots\dots\dots(10)$$

$$I_{s1} = -I_{s2} + \frac{(1 - n)V_o}{L_s} \Delta_1 T_s \dots\dots\dots(11)$$

$$I_{L1} = -I_{L2} + \frac{V_o}{L_1} \Delta_1 T_s \dots\dots\dots(12)$$

From (8), (9), (11), and (12), the maximum current of the output diode  $I_{Do}$  can be obtained by,

$$I_{Do} = I_{in} + I_{s1} + I_{L1} = \left( \frac{1 - n}{L_s} + \frac{1}{L_1} \right) V_{in} D T_s \dots\dots\dots(13)$$

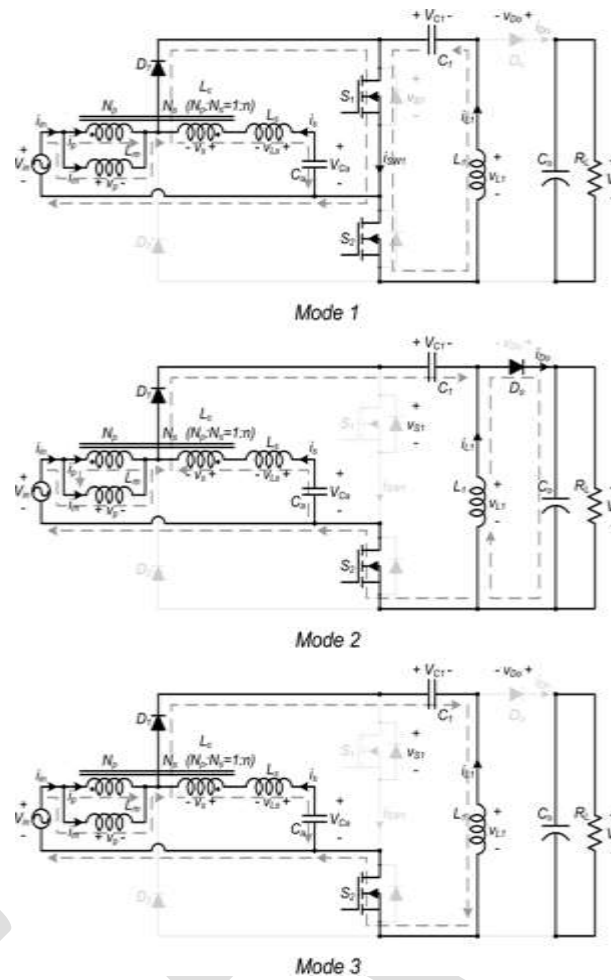


Fig 4. Operating modes

### III. SIMULATION MODELS

Simulation model of bridgeless SEPIC converter is implemented in MATLAB/Simulink environment and simulation results are verified. The bridgeless configuration reduces the number of switches leading to better efficiency. Moreover, the conduction losses are reduced and better performance is achieved. The torque ripples are eliminated and the power quality is improved especially the power factor is maintained at unity.

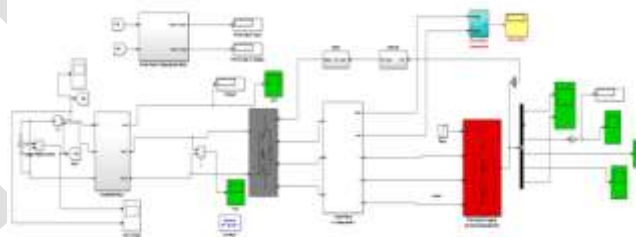


Fig.5 Simulation circuit for BLDC with modified SEPIC converter

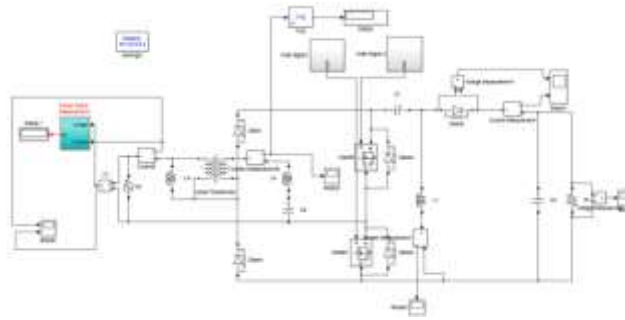


Fig .6 Simulation circuit for SEPIC

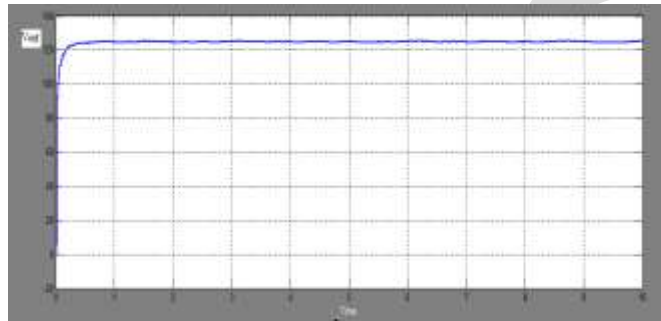


Fig. 7 Simulation result for input of SEPIC converter

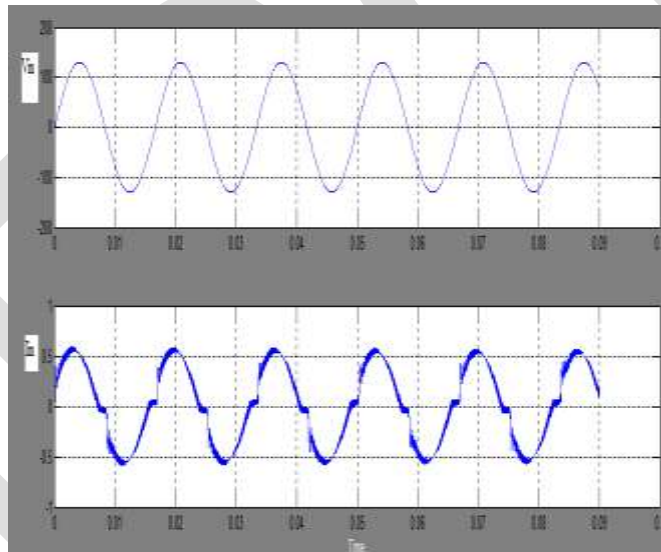


Fig. 8 Simulation result for output of SEPIC converter

#### IV. CONCLUSION

The conduction losses in the conventional SEPIC converter is high, this can be overcome by bridgeless SEPIC converter. The ripple current in the input side can reduce by bridgeless SEPIC converter. The final efficiency of PMBLDC can increase by using this converter and power factor can also increase.

#### REFERENCES:

- [1] Jae-Won Yang and Hyun-Lark Do, "Bridgeless SEPIC Converter With a Ripple-Free Input Current" *IEEE Trans. On Power Electronics*, Vol. 28, No. 7, July 2013.
- [2] L. Huber, Y. Jang, and M. M. Jovanovic, "Performance evaluation of bridgeless PFC boost rectifiers," *IEEE Trans. Power Electron.*, vol. 23, no. 3, pp. 1381–1390, May 2008.

- [3] Joseph.S, Ravi.A, Jasper Gnana Chandran, “Efficient Bridgeless SEPIC Converter for BLDC Motor with Improved Power Factor” *International Journal of Advanced Research in Electrical, Electronics and Instrumentation Engineering*
- [4] S.Assly Steffy, B.Mangaiyarkarasi, S.Sherin Jasper, K.Priyanka, K.Soorya, “Analysis And Simulation Of Speed Control Of PMBLDC motor by PI Controller” *International Journal of Advanced Research in Computer and Communication Engineering Vol. 3, Issue 2, February 2014*
- [5] Mr. V. Sarankumar, Mr. M. Murugan, Mr. R. Jeyabharath,“ Implementation of blsepic converter fed bldc motor drive with power factor rectification” *International Journal of Advanced Research in Computer and Communication Engineering Vol. 3, Issue 2, February 2014*
- [6] C.Umayal, D.Saranya Devi, “Modeling and Simulation of PFC SEPIC Converter fed PMBLDC Drive for Mining Application” *International Journal of Advanced Trends in Computer Science and Engineering, Vol.2 , No.2, Pages : 203- 208 (2013).*
- [7] Dr.T. Govindaraj1, H.Ashtalakshmi, “simulation of bridgeless sepic Converter with power factor Correction fed dc motor” *international journal of innovative research in electrical, electronics, instrumentation and control engineering Vol. 2, Issue 1, January 2014*